A Simple Dynamic Engine Model for Use in a Real-Time Aircraft Simulation With Thrust Vectoring

Steven A. Johnson

OCTOBER 1990

NASA

A Simple Dynamic Engine Model for Use in a Real-Time Aircraft Simulation With Thrust Vectoring

Steven A. Johnson
Ames Research Center
Dryden Flight Research Facility
Edwards, California

A SIMPLE DYNAMIC ENGINE MODEL FOR USE IN A REAL-TIME AIRCRAFT SIMULATION WITH THRUST VECTORING

Steven A. Johnson*
NASA Ames Research Center
Dryden Flight Research Facility
Edwards, California

Abstract

A simple dynamic engine model was developed at the NASA Ames Research Center, Dryden Flight Research Facility, for use in thrust vectoring control law development and real-time aircraft simulation. The simple dynamic engine model of the F404-GE-400 engine (General Electric, Lynn, Massachusetts) operates within the aircraft simulator. It was developed using tabular data generated from a complete nonlinear dynamic engine model supplied by the manufacturer. Engine dynamics were simulated using a throttle rate limiter and low-pass filter. This paper includes a description of a method to account for axial thrust loss resulting from thrust vectoring. In addition, this paper presents the development of the simple dynamic engine model and its incorporation into the F-18 high alpha research vehicle (HARV) thrust vectoring simulation. The simple dynamic engine model was evaluated at Mach 0.2, 35,000-ft altitude and at Mach 0.7, 35,000-ft altitude. The simple dynamic engine model is within 3 percent of the steady state response, and within 25 percent of the transient response of the complete nonlinear dynamic engine model.

Nomenclature

$A8$	nozzle throat area, in^2
$CFGX$	axial thrust ratio, $\dfrac{FG_{(axial)}}{FG}$
D_{inl}	inlet spillage drag, lbf
D_{noz}	nozzle aft-end drag increment, lbf
FG	gross thrust, lbf
$FG_{(axial)}$	axial gross thrust after thrust vectoring, lbf
FNP	net propulsive force, lbf
F_{ram}	ram drag, lbf
GE	General Electric
H	altitude, ft
HARV	high alpha research vehicle
Max AB	maximum afterburner
Min AB	minimum afterburner
Mil power	intermediate-rated power
NPR	nozzle pressure ratio
PLA	power lever angle, deg
PLA$'$	shaped power lever angle, deg
TVCS	thrust vectoring control system
alpha	angle of attack
τ	time constant, sec

Introduction

The National Aeronautics and Space Administration (NASA) has undertaken a program to investigate the high-angle-of-attack flight regime with a modified F-18 aircraft called the high alpha research vehicle (HARV).[1] Some of the modifications to the F-18 HARV include adding a simple thrust vectoring system that employs turning vanes located aft of the engine primary nozzles. These vanes will be used to fly and sustain the F-18 HARV to angles of attack in excess of 70°. To use the thrust vectoring turning vanes

to control the aircraft, modifications to the aircraft control laws were necessary.

In support of these control law modifications, there was a need for a real-time dynamic model of the F-18 engine, the F404-GE-400 (General Electric, Lynn, Massachusetts). The model would operate in the NASA Ames Research Center, Dryden Flight Research Facility's F-18 HARV simulator. An attempt was made to incorporate the engine manufacturer's nonlinear component level dynamic engine model (General Electric Report R88AEB427, *Software User's Manual for the HARV F404-GE-400 Dynamic Real Time Model*) into the simulation, but execution time constraints of the F-18 HARV simulation prohibited its use. As a result, development began on a simple dynamic engine model that would execute within the control law execution rate; perform within 5 percent of the steady state response, and perform within 25 percent of the transient response of the complete nonlinear component level dynamic engine model. In addition, the thrust vectoring effect on the axial thrust of the aircraft needed to be accounted for in the engine model.

A simple dynamic engine model was developed that fulfilled the timing and accuracy requirements for control law development and evaluation. The simple dynamic engine model includes tables of internal engine parameters that were generated using the engine manufacturer's nonlinear component level dynamic engine model. Tables of engine–aircraft installation effects parameters were generated using a simple model from the airframe manufacturer. Engine dynamics were simulated using a throttle rate limiter and low-pass filter.

This paper provides an overview of the development of the simple dynamic engine model. It presents a comparison of the model results to the engine manufacturer's complete nonlinear component level dynamic engine model at two typical thrust vectoring flight conditions. In addition, there is a description of the engine model's incorporation into the F-18 HARV thrust vectoring simulation.

Vehicle and Model Description

Vehicle Description

The F-18 HARV (Fig. 1) is a single-place aircraft built by the McDonnell Douglas (St. Louis, Missouri) and Northrop (Newbury Park, California) Corporations. The aircraft features a midwing with leading-

and trailing-edge flaps. Leading-edge extensions are mounted on each side of the fuselage from the wing roots to just forward of the windscreen. The aircraft has twin vertical stabilizers canted out from vertical 20° and differential all-moving horizontal tails.

The F-18 HARV is powered by two F404-GE-400 engines. The F404-GE-400 engine is a 16,000-lb thrust class, low bypass, twin spool turbofan with afterburner. It incorporates a three-stage fan and a seven-stage high-pressure compressor, each driven by a single-stage turbine.[2] During flight, power lever angle (PLA) ranges from 31° (flight idle) to 130° (full power with afterburner). Intermediate power (full nonafterburning) occurs at 87° PLA.

The F-18 HARV is being modified to incorporate a simple multiaxis thrust vectoring control system (TVCS) as shown in Fig. 2. Figure 2(a) shows the installation details of the six thrust vectoring vanes to be installed on the aft fuselage. With installation of the TVCS, the divergent portion of the nozzle and the external nozzle flaps will be removed from the engines. The circumferential and radial locations of the vanes relative to the nozzle exit are shown in Fig. 2(b). The vanes are double curvature in shape and are limited to a deflection range of −10° out of the jet exhaust to +25° into the jet exhaust (Fig. 2(c)).

Model Description

Real-time simulation of the F-18 HARV aircraft required a simple dynamic engine model that fulfilled the timing and accuracy requirements for control law development and evaluation. A simple dynamic engine model was developed using data from a nonlinear component level dynamic engine model, an engine–aircraft installation effects model, and a model of the thrust vectoring performance of the F-18 HARV vane configuration. Figure 3 is a schematic of the models used to develop the various parts of the simple dynamic engine model. A description of these models and the resulting simple dynamic engine model follows.

Nonlinear Component Level Dynamic Engine Model. Complex nonlinear dynamic engine models developed by the engine manufacturer provide accurate engine values for the F404-GE-400 engine. An example is the GE Dynamic Real Time Model–a low-frequency, transient aerothermodynamic turbofan simulation (General Electric Report R88AEB427, *Software User's Manual for the HARV F404-GE-400 Dynamic Real Time Model*). Each engine compo-

nent (fan, core compressor, combustor, turbines, afterburner, nozzle) is mathematically modeled within the body of the overall model. The GE model includes the F-18 HARV nozzle modifications which affect the gross thrust value.

The GE model is coupled with the airframe manufacturer's engine–airframe installation effects model which estimates inlet drag as a function of Mach number and spillage airflow. The data for this model were derived from force and moment testing of a 6-percent scale model of a production F-18 aircraft. In addition, the model estimates nozzle aft-end drag increment as a function of Mach number, altitude, and PLA. This increment is added to the baseline nozzle aft-end drag of a production F-18 aircraft. The nozzle modification makes this increment unique to the F-18 HARV aircraft.

The GE engine modeling process uses a set of simultaneous nonlinear equations that cannot be solved closed form. As a result, iteration techniques are used to converge on a solution. The GE Dynamic Real Time Model coupled with the engine–airframe installation effects model contains approximately 6,250 lines of FORTRAN code. For a 20-msec time frame, the GE model requires approximately 4 msec to execute on a Gould Sel 97 (Gould Incorporated, Computer Systems Division, Fort Lauderdale, Florida) simulation computer. In addition, the GE model is designed to execute additional time steps to remain in phase with the external simulation time step. These additional time steps further increase the model execution time. For a 40-msec time frame, the model requires approximately 12 msec to execute. The F-18 aircraft simulation at NASA Ames-Dryden had execution time constraints that prohibited the use of the GE Dynamic Real Time Model.

Simple Dynamic Engine Model. Because of the execution time constraints, a simple dynamic engine model was developed that used a different modeling approach. Instead of using equations to model each individual engine component, tabular data of steady state values of gross thrust (FG), ram drag (F_{ram}), nozzle pressure ratio (NPR), and nozzle throat area $(A8)$ data were used. The tables were generated using the GE Dynamic Real Time Model for standard day conditions. All tabular data are the same size and are a function of Mach number, altitude, and PLA. The breakpoints of Mach number and altitude are shown in Fig. 4.

Breakpoints of PLA are flight idle, intermediate-rated power (Mil power), minimum afterburner (Min AB), and maximum afterburner (Max AB). An example plot of the gross thrust tabular data values appears in Fig. 4. The plot symbols represent the table values of Max AB gross thrust at different Mach number and altitude conditions for the F404-GE-400 engine with the modified F-18 HARV nozzle.

The simple dynamic engine model also includes tabular data of steady state values of inlet spillage drag (D_{inl}) and nozzle aft-end drag increment (D_{noz}). These tables were generated using the airframe manufacturer's engine–airframe installation effects model and are a function of the same parameters as the engine tabular data generated from the GE Dynamic Real Time Model.

Engine Dynamics Model Description

A thrust vectoring aircraft simulation with a variable throttle requires an accurate model of the engine parameter dynamics. A study examining the response of the GE Dynamic Real Time Model to throttle steps showed that the engine parameters required for this simulation exhibited approximately a first-order response. The study showed that the transient response of the engine parameters from a Min AB to Max AB throttle step was faster than the transient response from a flight idle to Mil power throttle step. In addition, a faster response was noted when stepping the throttle from high to low power rather than from low to high power. Lastly, the transient response of these engine parameters changed only slightly with typical thrust vectoring flight conditions. The results implied that it was feasible to develop a simple model to introduce engine parameter dynamics.

A simple model was developed that introduced dynamics to the engine model by routing the PLA cockpit command through a low-pass filter and a rate limiter. Using this method, the dynamics introduced to the PLA modifies the response of all tabular engine parameters. A block diagram of the PLA shaping model appears in Fig. 5. Both the low-pass filter time constant and rate limiter are a function of power zone. These values were determined by averaging the best-fitting rate limiters and time constants to gross thrust at the four corners of the F-18 HARV flight envelope. When stepping the throttle from high to low power, it was noted that the pure first-order decay sufficiently modeled engine parameter dynamics. As a result, there is no rate limiting on decreasing PLA.

3

Thrust Loss Resulting From Vectoring

The F-18 HARV TVCS aircraft simulation contains a thrust vectoring performance model that uses internal engine parameters in the calculation of thrust vectoring performance. The simple dynamic engine model supplies these parameters. The thrust vectoring performance model was developed from results of a 14.25-percent scale static nozzle test performed in the static test facility of the NASA Langley Research Center 16-Foot Transonic Tunnel.

During the NASA Langley static nozzle test, one of the parameters investigated was the amount of axial thrust lost as a result of vane deflection. This parameter, $CFGX$, is defined as the ratio of the thrust along the body axis to the undeflected gross thrust. As the turning vanes are deflected into the jet exhaust, axial thrust is lost as a result of both the turning of the gross thrust vector and the friction and pressure drags associated with the thrust vectoring hardware.[3] As shown in Fig. 6, the static nozzle test results indicate that axial thrust loss, caused by vane deflection, has a significant effect on the axial thrust of the aircraft (FNP). The example presented uses results from the thrust vectoring performance model and thrust values from the simple dynamic engine model. This illustrates the effect of axial thrust loss as a result of thrust vectoring on FNP for each engine. This effect is evaluated at a typical F-18 HARV flight condition (Mach 0.2 and 35,000-ft altitude). As the inboard and outboard vanes are deflected 25° into the flow and the top vane is fixed at −10°, for each engine as much as 1,000 lb of axial thrust are lost because of the turning of the gross thrust vector and the vane friction and pressure losses.

Model Incorporation Description

Figure 7 represents the overall schematic of the simple dynamic engine model. As illustrated, input parameters to the simple dynamic engine model are determined from the aircraft simulation flight condition and cockpit PLA position. As described previously, simple dynamics are introduced to engine parameters by shaping the cockpit PLA command. The values of FG, F_{ram}, D_{inl}, D_{noz}, NPR, and $A8$ are determined by linearly interpolating the tabular data with respect to altitude, Mach number, and shaped power lever angle (PLA').

Figure 7 also illustrates how the simple dynamic engine model interfaces with the thrust vectoring performance model and control laws. In addition, it shows how FNP is determined using the tabular en-

gine parameters, engine–airframe installation effects parameters, and $CFGX$. Net propulsive force is used as the axial thrust component in the aircraft simulation equations of motion.

Results

Comparison With the General Electric Dynamic Real Time Model

The accuracy of the simple dynamic engine model was evaluated by comparing it to the GE Dynamic Real Time Model. Data presented are for one engine only. Identical input conditions were used by both models to examine and compare the output of the models. A standard PLA input time history was used, which consisted of the PLA set to flight idle at 0 sec. At 7 sec, the PLA was stepped to Mil power. At 14 sec, the PLA was stepped to Max AB. At 21 sec, the PLA was stepped to Min AB. At 28 sec, the PLA was stepped to flight idle, and at 35 sec the input time history was terminated.

An input technique of this manner was chosen because it exercised all the different time constants and rate limiter values of the simple dynamic engine model. In addition, it showed both the steady state and dynamic responses of the models. This PLA input time history was evaluated for two flight cases at the two upper corners of the F-18 HARV design envelope. These two conditions were chosen because they represent typical flight conditions for an aircraft with thrust vectoring. The first case was at Mach 0.2 and 35,000-ft altitude; the second case was at Mach 0.7 and 35,000-ft altitude.

Figure 8 shows a comparison of the standard PLA input to the PLA'. As with the case of increasing PLA, the PLA rate limiter is in effect in the simple dynamic model. This results in a PLA rate of increase that is less than the first-order response rate of increase. In areas of decreasing PLA, no PLA rate limiter is in effect, and the first-order decay of the PLA response is evident.

Comparisons at First Flight Case. Figure 9 shows comparisons of the simple dynamic engine model with the GE Dynamic Real Time Model at Mach 0.2 and 35,000-ft altitude. Figure 9(a) shows the PLA input time history used for both models while Figs. 9(b)–9(e) show the output time history comparisons.

Figure 9(b) shows the gross thrust time history comparison of the models. Only slight differences are dis-

cernible in steady state FG responses of both models. In examining the dynamic responses of the models–for the case of increasing gross thrust–the PLA rate limiter is in effect in the simple dynamic model. By limiting the PLA rate of increase, the FG rate of increase is nearly the same as the GE model FG. The largest difference in the rate of change between models is seen at 8 sec. At this transient condition, the simple dynamic model FG is approximately 20 percent less than the GE model FG. In areas of decreasing thrust, no PLA rate limiter is in effect, and the first-order decay of the simple dynamic model closely matches the gross thrust response of the GE model.

Figure 9(c) shows the net propulsive force time history comparison of the models with no thrust vectoring. Net propulsive force is calculated by subtracting ram drag, inlet spillage drag, and nozzle aft-end drag increment from gross thrust. Note that the steady state and dynamic differences between the models are similar to those seen in Fig. 9(b). At this low Mach number, the magnitude of F_{ram}, D_{inl}, and D_{noz} is small. As a result, the steady state magnitude of FNP with no vectoring is within 250 lb of the FG values presented in Fig. 9(b). As shown in Fig. 5, thrust vectoring would result in axial thrust loss, a decrease in FNP, and an increase in the steady state differences between FG and FNP.

Figures 9(d)–9(e) show the nozzle pressure ratio and nozzle throat area time history comparison of the models. The GE Dynamic Real Time Model schedules $A8$ as a function of: PLA, ambient pressure, fan rotor speed, exhaust gas temperature, and inlet total temperature.[2] At a flight idle PLA, $A8$ is scheduled to a throat area of 400 in^2. As the PLA is advanced to Mil power, the nozzle closes and $A8$ is reduced. This results in an increase in NPR. As PLA advances from Mil power to afterburner operation, $A8$ opens to maintain the exhaust gas temperature within limits, resulting in little change in the NPR response. In examining the dynamic response of NPR, the greatest difference in the rate of change between models is seen at 8 sec. At this transient condition, the simple dynamic engine model NPR is 18 percent less than the GE model NPR. In areas of decreasing NPR, the pure first-order decay of the simple dynamic engine model closely matches the NPR response of the GE Dynamic Real Time Model.

Figure 9(e) shows the nozzle throat area time history comparison of the models. Because five different parameters influence the GE model $A8$, it is the most difficult parameter to model with the technique used in the simple dynamic engine model. As seen in Fig. 9(e), the steady state responses of both models are nearly identical. In examining the dynamic responses of the models, the change between PLA settings has the GE Dynamic Real Time Model $A8$ closing and opening faster than the simple dynamic engine model $A8$. This is because the time constants and PLA rate limiters of the simple dynamic engine model are designed for the gross thrust rate of change but not the $A8$ rate of change. A very accurate model of the nozzle throat area was beyond the scope of this study, but adding tables at more PLA settings and developing $A8$ specific rate limiters and time constants would increase the accuracy of $A8$. The largest difference in the rate of change between models is seen at 8 sec. At this transient condition, the simple dynamic engine model $A8$ is 25 percent greater than the GE model $A8$. However, at 8 sec gross thrust is only 2,000 lb, so there is little thrust to vector. As a result, the difference between models is not considered to have a significant impact on aircraft simulation performance with thrust vectoring.

Comparisons at Second Flight Case. Figure 10 illustrates comparisons of the simple dynamic engine model with the GE Dynamic Real Time Model at Mach 0.7 and 35,000-ft altitude. Figure 10(a) shows the PLA input conditions used for the models. The output time history comparisons are presented in Figs. 10(b)–10(e). Figure 10(b) shows the gross thrust time history comparison of the models. The steady state responses of both models compare favorably. For instance, the simple dynamic engine model FG is within 3 percent of the GE model FG at 25 sec. In examining the dynamic response of the models, the FG response of the simple dynamic engine model once again is in close agreement with the FG response of the GE Dynamic Real Time Model.

Figure 10(c) shows the net propulsive force time history comparison of the models. At this flight condition, the magnitude of F_{ram}, D_{inl}, and D_{noz} is appreciable. At the Max AB condition, the steady state magnitude of net propulsive force is 1,223 lb or 18.5 percent less than the gross thrust values presented in Fig. 10(b).

Figures 10(d)–10(e) show the NPR and $A8$ time history comparison of the models. The NPR and $A8$ responses at this flight condition show all of the Mach 0.2, 35,000-ft altitude response characteristics. Steady state differences between the models are al-

most negligible. In examining the dynamic response of the models, the nozzle pressure ratio response of the simple dynamic engine model once again is in close agreement with the nozzle pressure ratio response of the GE Dynamic Real Time Model. As at Mach 0.2, 35,000-ft altitude, the GE Dynamic Real Time Model nozzle throat area closes and opens faster than the simple dynamic engine model nozzle throat area.

Using tabular data of FG, F_{ram}, D_{inl}, D_{noz}, NPR, $A8$, a low-pass filter, and PLA rate limiter, these results demonstrate that the simple dynamic engine model closely matches the response of the GE Dynamic Real Time Model for the input conditions studied. As seen in the time history comparisons between models, the steady state differences of FG, FNP, NPR, and $A8$ are less than 3 percent; this is within the original goal of 5 percent. The differences between models in the transient responses of FG, FNP, and NPR are less than or equal to 20 percent. In $A8$ the difference was as much as 25 percent during the step from flight idle to Mil power.

Execution Time

As previously described, the modeling process of the simple dynamic engine model uses sets of tables that are linearly interpolated with aircraft flight condition and a PLA shaping model to add engine dynamics. Compared to the GE Dynamic Real Time Model which uses iteration to solve nonlinear equations, the simple dynamic engine model would be expected to have shorter execution times. For a 20-msec time frame, the simple dynamic engine model requires approximately 0.3 msec to execute on a Gould Sel 97 simulation computer. A larger simulation time step has no effect on the model execution time. The simple dynamic engine model contains approximately 25 percent of the lines of FORTRAN code and requires only 25 percent of the storage memory requirements of the GE Dynamic Real Time Model. The faster execution time and reduced storage requirements of the simple dynamic engine model allowed it to meet the interface and timing requirements of the F-18 HARV aircraft simulation at NASA Ames-Dryden.

Concluding Remarks

A simple real-time engine simulation was developed at NASA Ames Research Center, Dryden Flight Research Facility for use in thrust vectoring control law development and real-time aircraft simulation. The engine model contains tables of internal engine parameters that were generated using the engine manu-

facturer's nonlinear component level dynamic engine model. In addition, it includes tables of engine–aircraft installation effects parameters that were generated using a simple model from the airframe manufacturer. Engine dynamics were simulated using a throttle rate limiter and low-pass filter.

The accuracy of the response characteristics of the simple dynamic engine model was examined using the General Electric (GE) Dynamic Real Time Model at two typical thrust vectoring aircraft flight conditions. The simple dynamic engine model steady state response matched the GE Dynamic Real Time Model response within 3 percent at the conditions studied. In examining the overall dynamic responses of the models, the simple dynamic engine model transient response matched the GE Dynamic Real Time Model response within 25 percent at the conditions studied. For gross thrust (FG), net propulsive force (FNP), and nozzle pressure ratio (NPR) the model transient responses were within 20 percent of each other. These results were within the original accuracy goal for the simple dynamic engine model.

The execution times of the models were determined. Both engine models were executed on a Gould Sel 97 (Gould Incorporated, Computer Systems Division, Fort Lauderdale, Florida) simulation computer. For a 20-msec time frame, the simple dynamic engine model took approximately 0.3 msec to execute, compared to 4 msec for the GE Dynamic Real Time Model. These results verify that fast execution and engine parameters with the required accuracy are being achieved with the F-18 high alpha research vehicle, thrust vectoring control system (HARV TVCS) simple dynamic engine model.

References

[1] Gilbert, William P., Luat T. Nguyen, and Joseph Gera, *Control Research in the NASA High-Alpha Technology Program*, AGARD Fluid Dynamics Panel Symposium on Aerodynamics of Combat Aircraft Control and of Ground Effects, Oct. 1989.
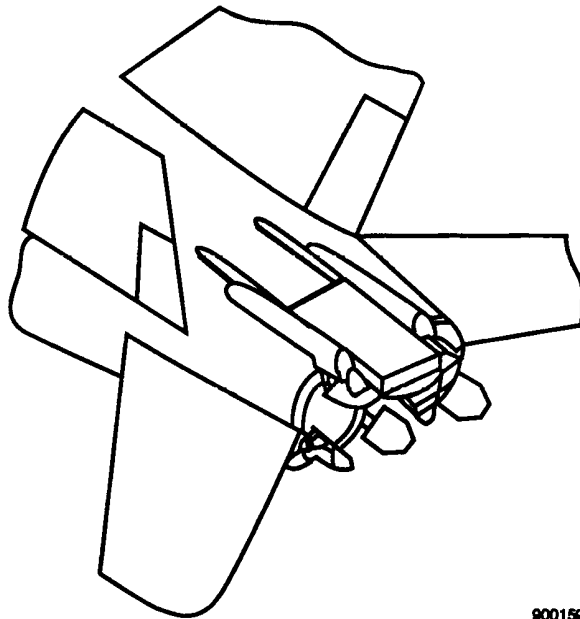
[2] *F404-400 Training Guide*, SEI-477, GE Aircraft Engines, 1989.

[3] Berrier, Bobby L., and Mary L. Mason, *Static Performance of an Axisymmetric Nozzle With Post-Exit Vanes for Multiaxis Thrust Vectoring*, NASA TP-2800, 1988.
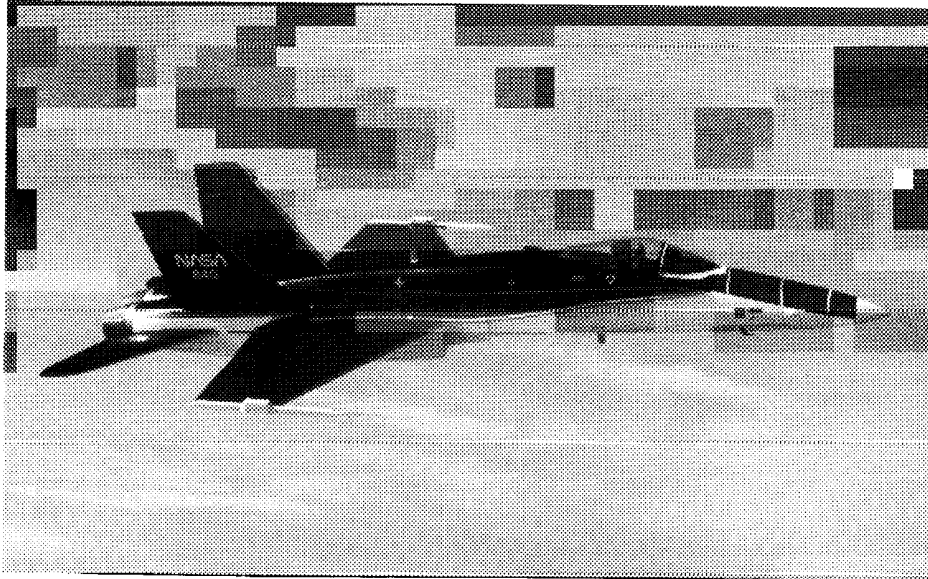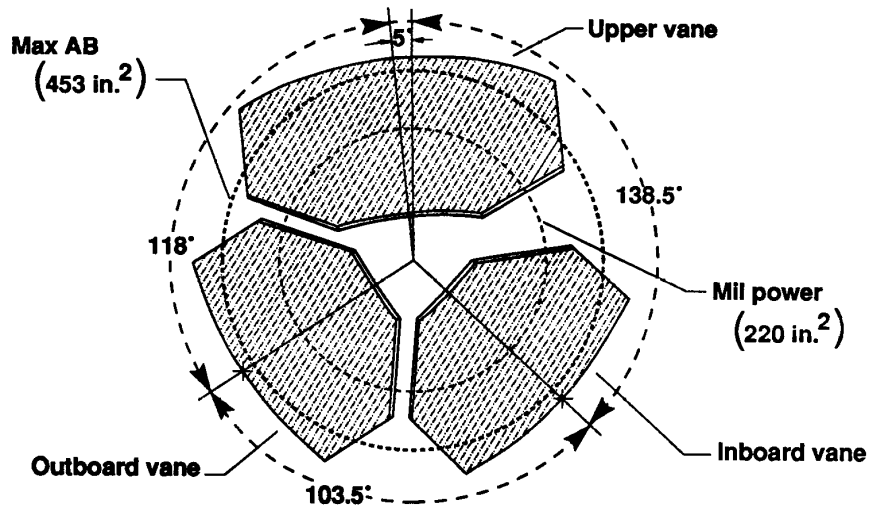
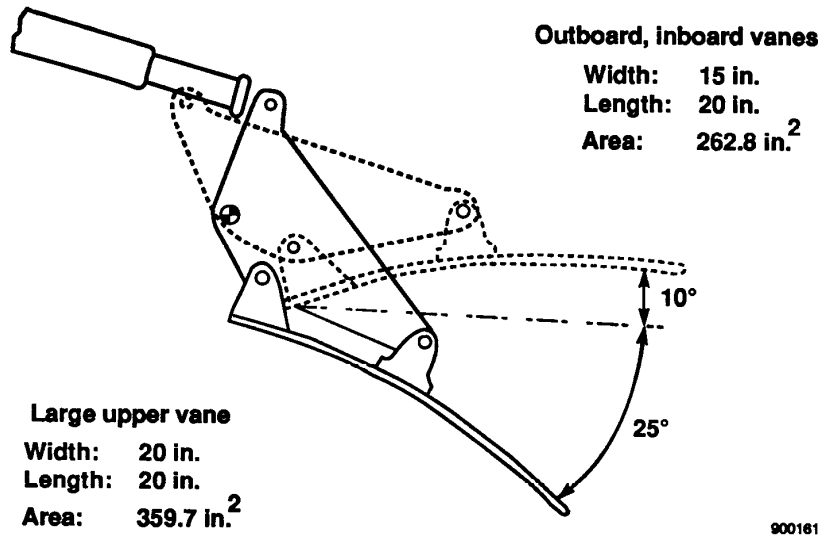EC 89-0062-001

Fig. 1 F-18 HARV.

900159

(a) Installation details of the six turning vanes.

Fig. 2 F-18 HARV vane configuration.

7

Max AB
$\left(453 \text{ in.}^2\right)$

Upper vane

138.5°

118°

Mil power
$\left(220 \text{ in.}^2\right)$

Outboard vane

Inboard vane

103.5°

900160

(b) Vane positions shown fully deflected.

Outboard, inboard vanes

Width: 15 in.
Length: 20 in.
Area: 262.8 in.^{2}

10°

25°

Large upper vane

Width: 20 in.
Length: 20 in.
Area: 359.7 in.^{2}

900161

(c) Vane geometry and deflection range.

Fig. 2 Concluded.

8
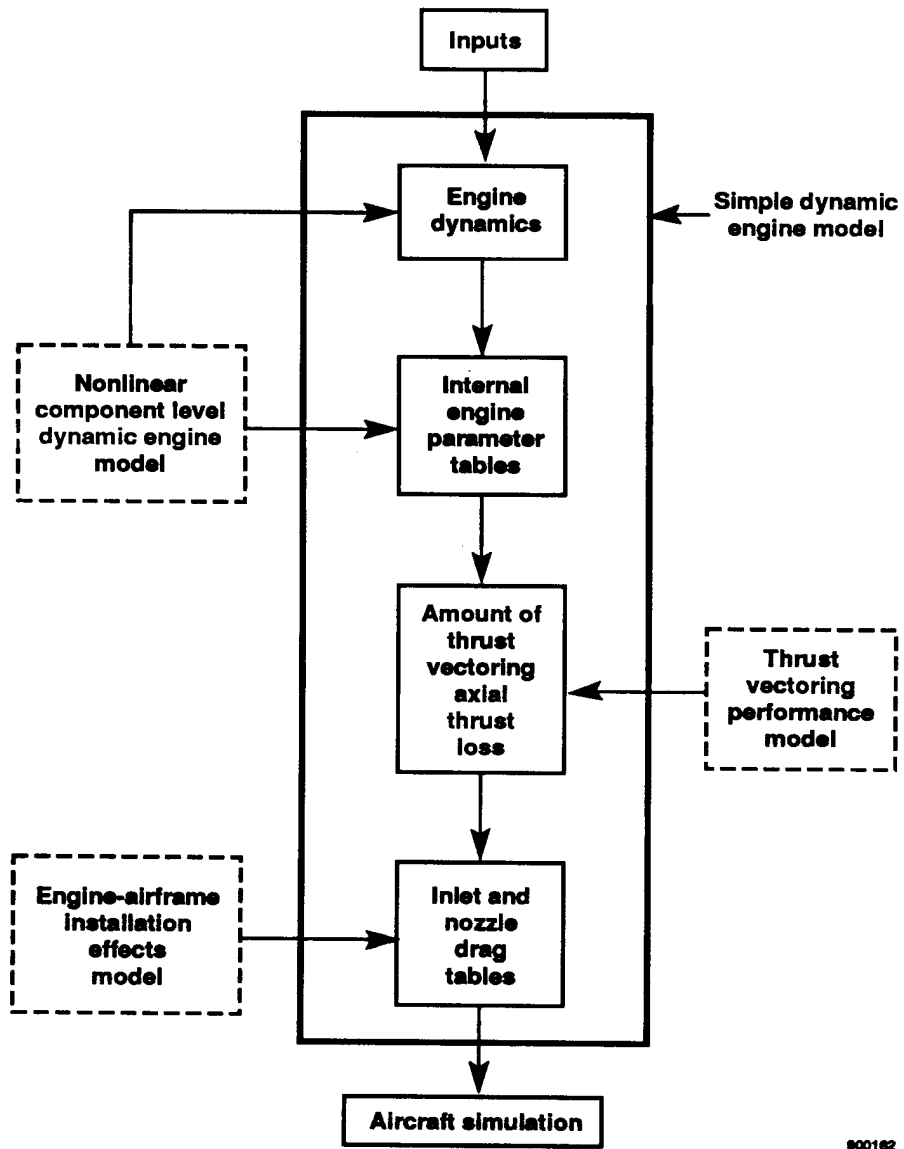
Fig. 3 Schematic of the models used in the development of the simple dynamic engine model.
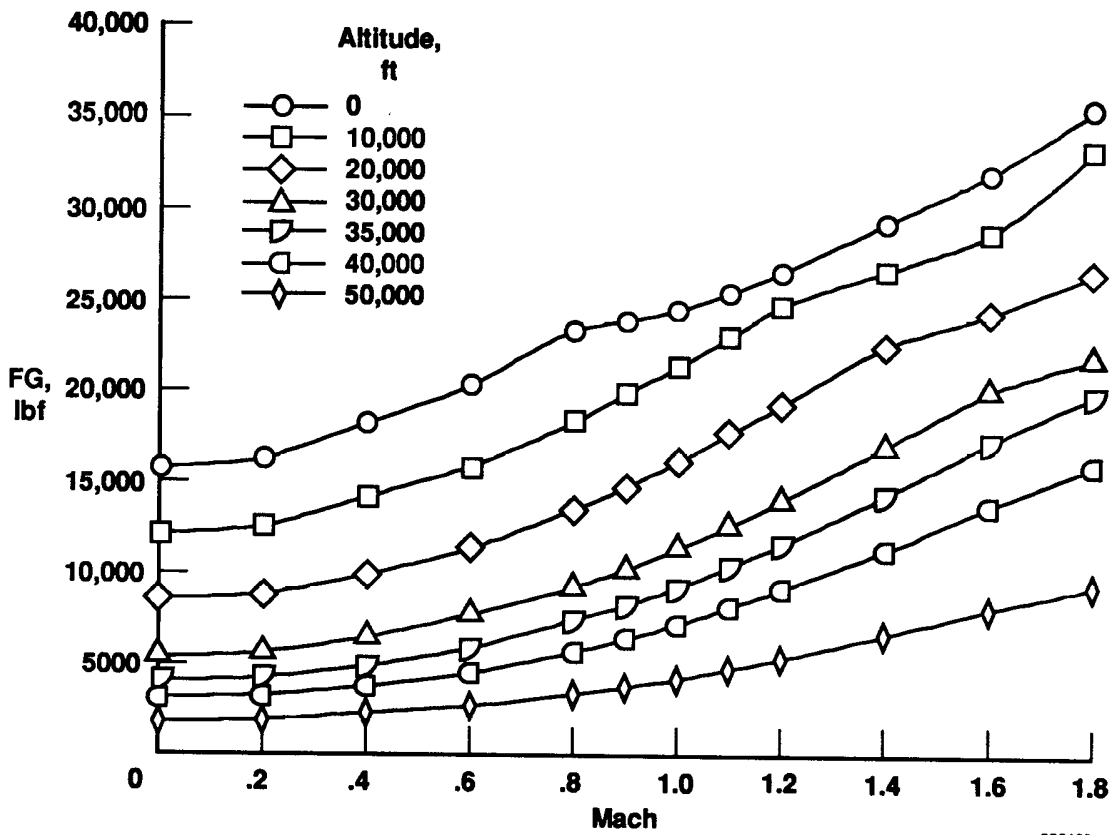
Fig. 4 Max AB gross thrust tabular data.
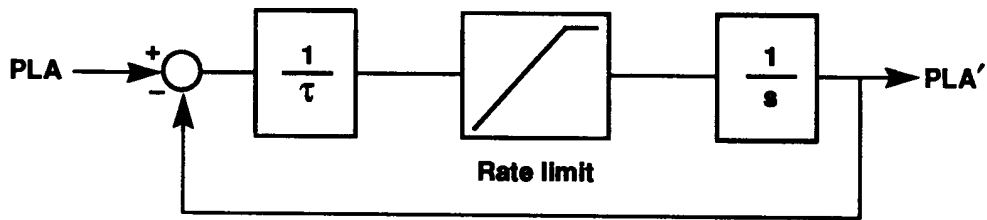
τ nonafterburning = 0.625 sec

τ afterburning = 0.550 sec

Rate limit nonafterburning = + 19.03 deg/sec

Rate limit afterburning = + 26.81 deg/sec

900164

Fig. 5 PLA shaping model block diagram.
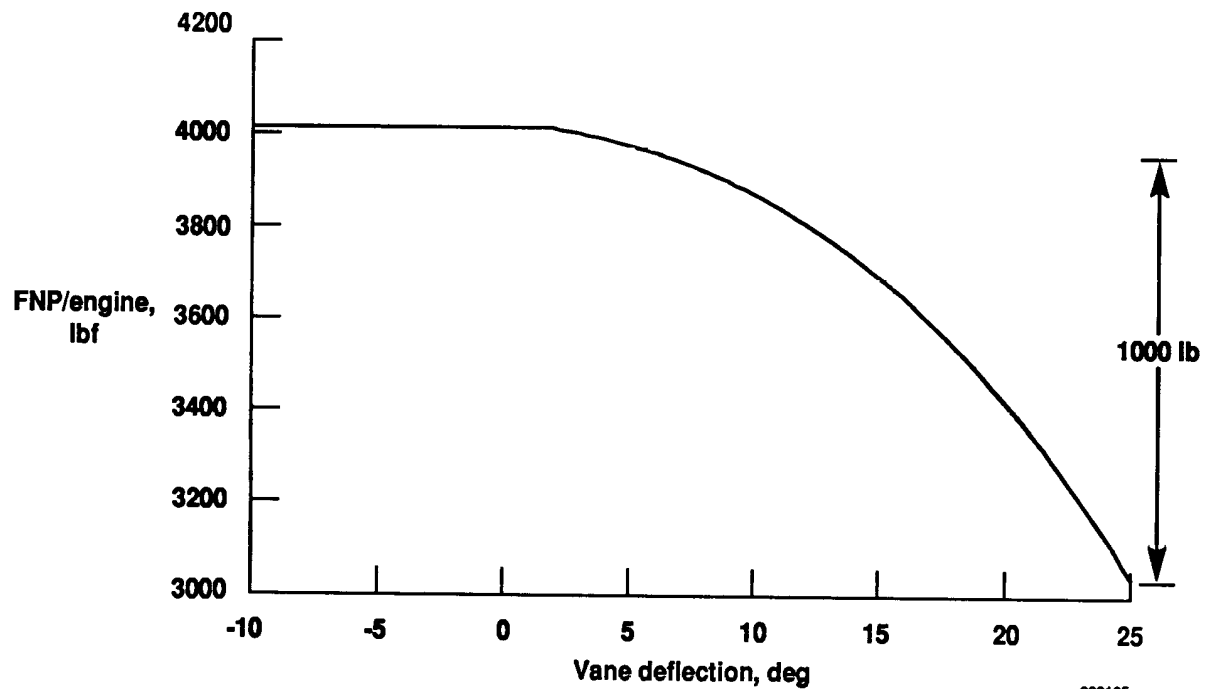
900165

Fig. 6 Reduction of FNP for each engine caused by thrust vectoring. Symmetric inboard- and outboard-vane deflection, $-10°$ top vane, Mach 0.2, $H = 35,000$ ft, Max AB.

11
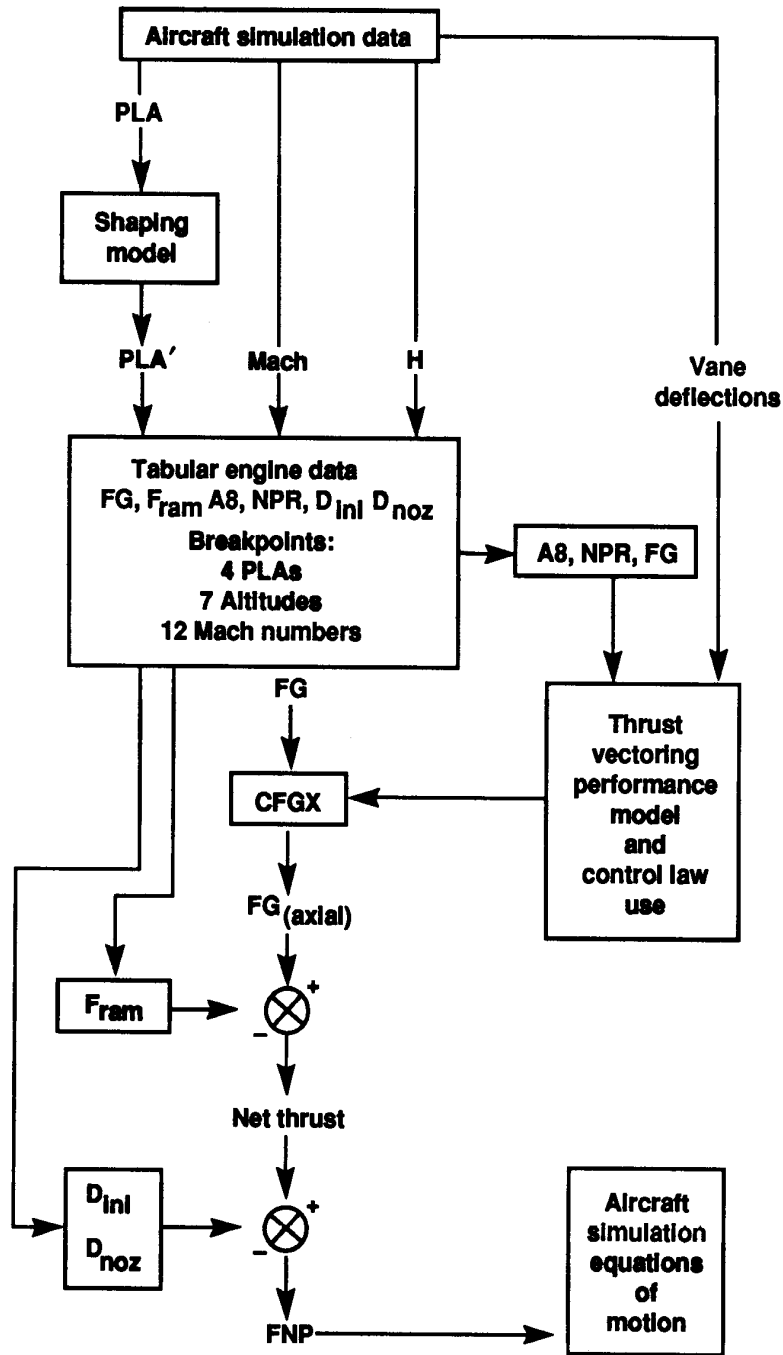
Fig. 7 Schematic of the simple dynamic engine model and its incorporation into the thrust vectoring simulation.
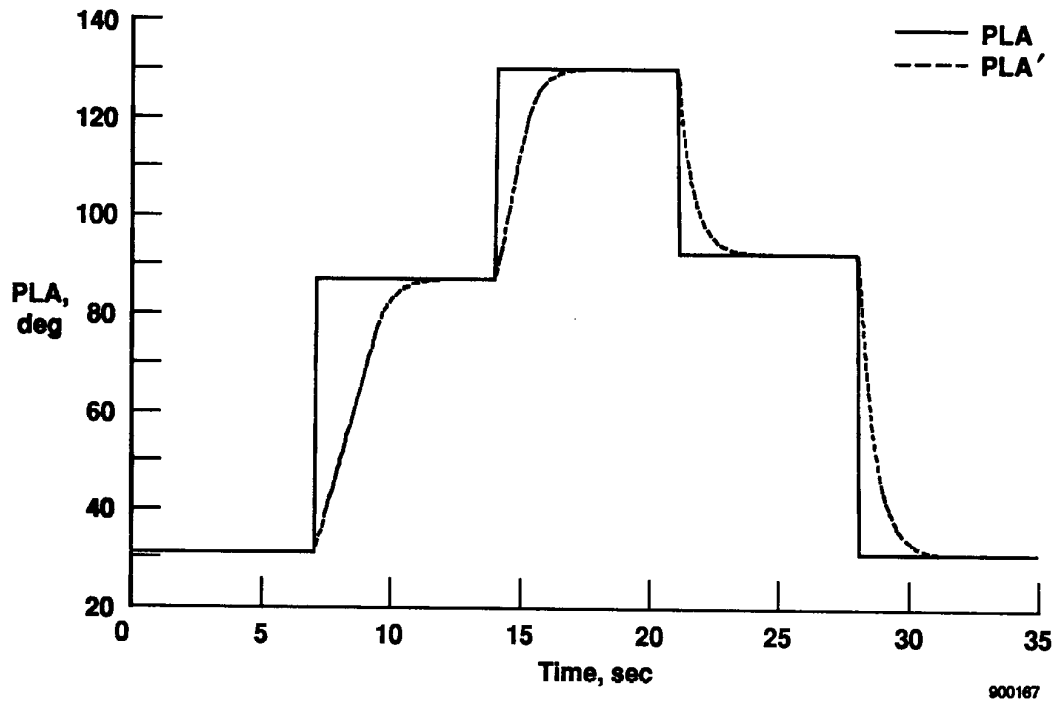
Fig. 8 Comparison of the standard PLA input and the resulting simple dynamic engine model PLA response.

13
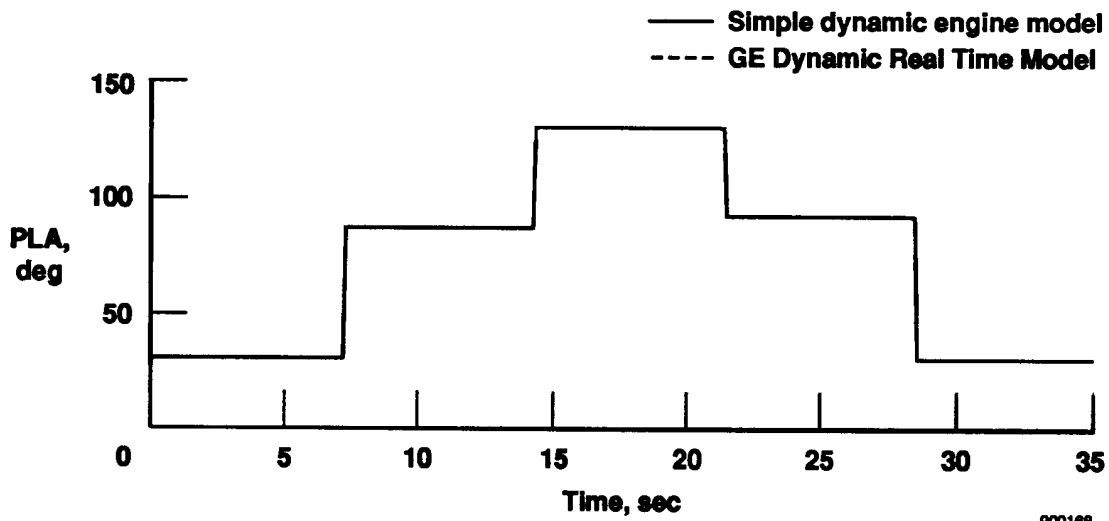
(a) Power lever angle input condition.
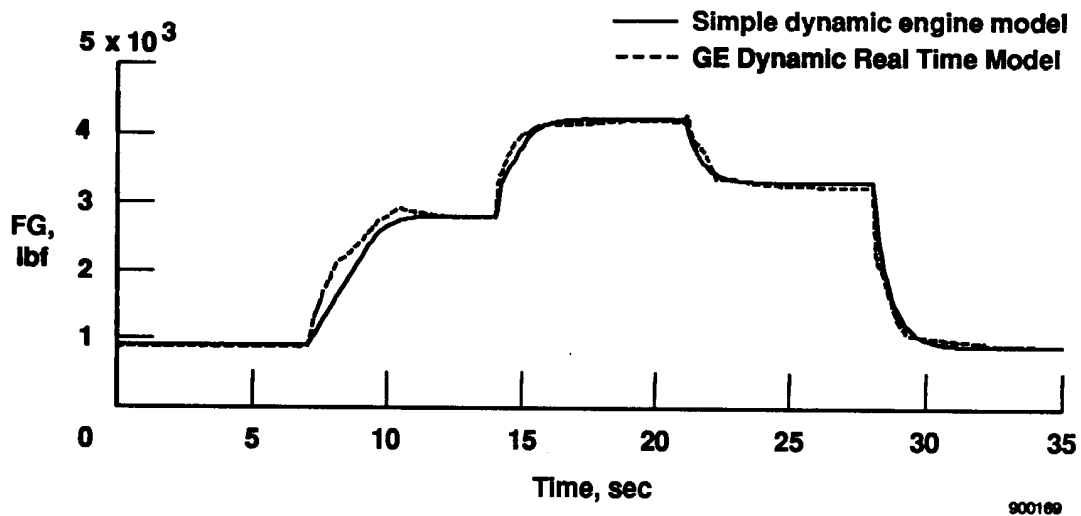
(b) Gross thrust comparison.

Fig. 9 Comparison of the simple dynamic engine model parameters and the GE Model engine parameters, Mach 0.2, H = 35,000 ft, no vectoring.

14
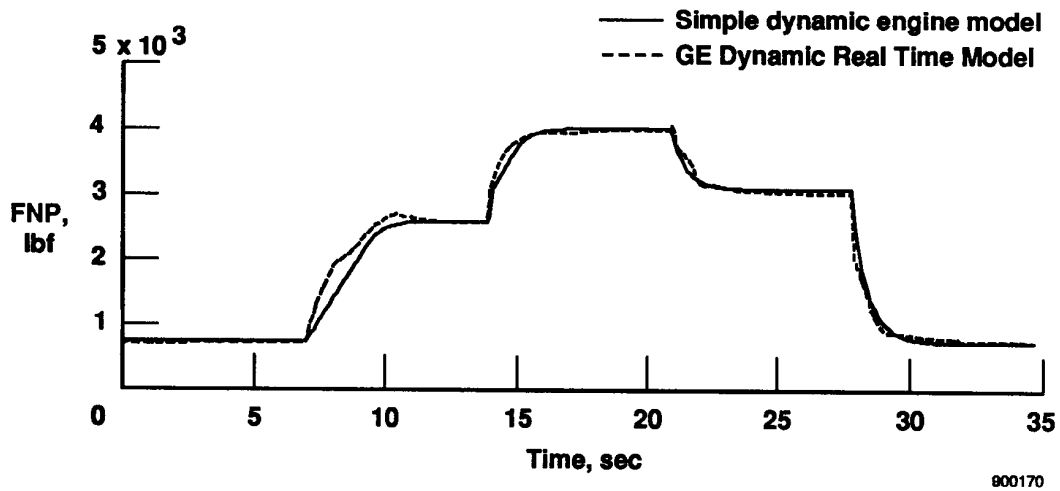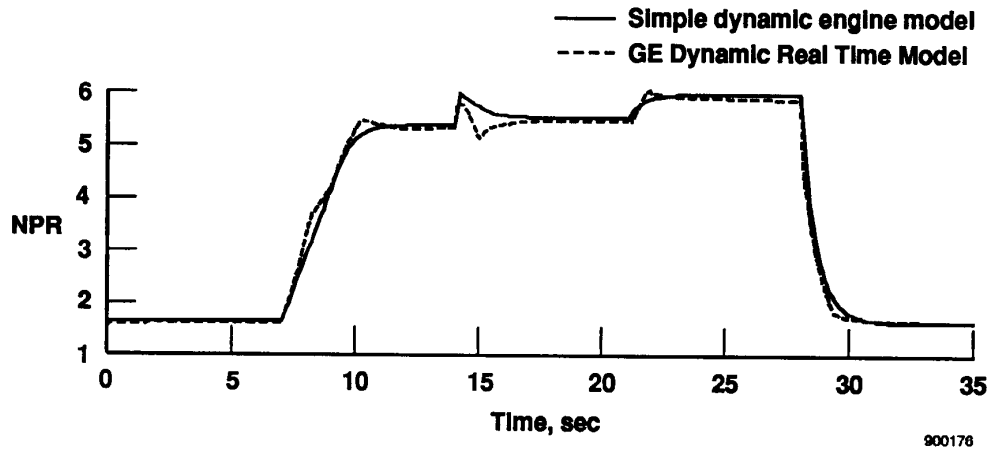
(c) Net propulsive force comparison.
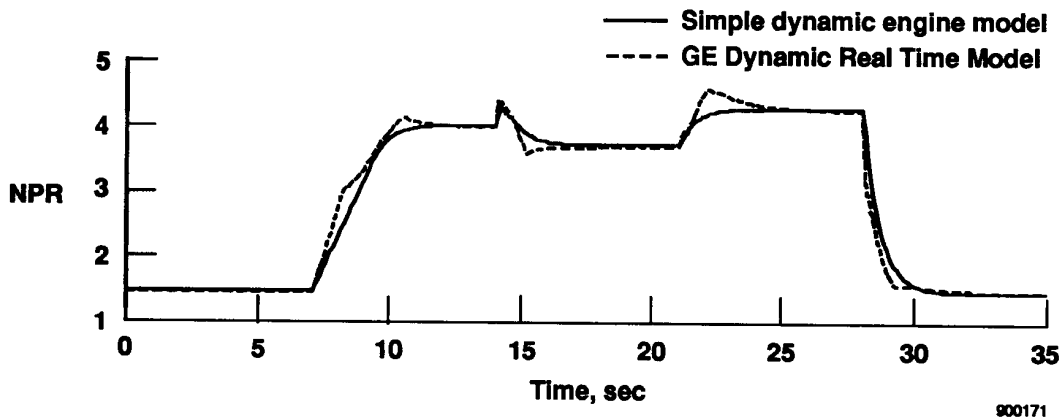
900170

(d) Nozzle pressure ratio comparison.

Fig. 9 Continued.

900171

15
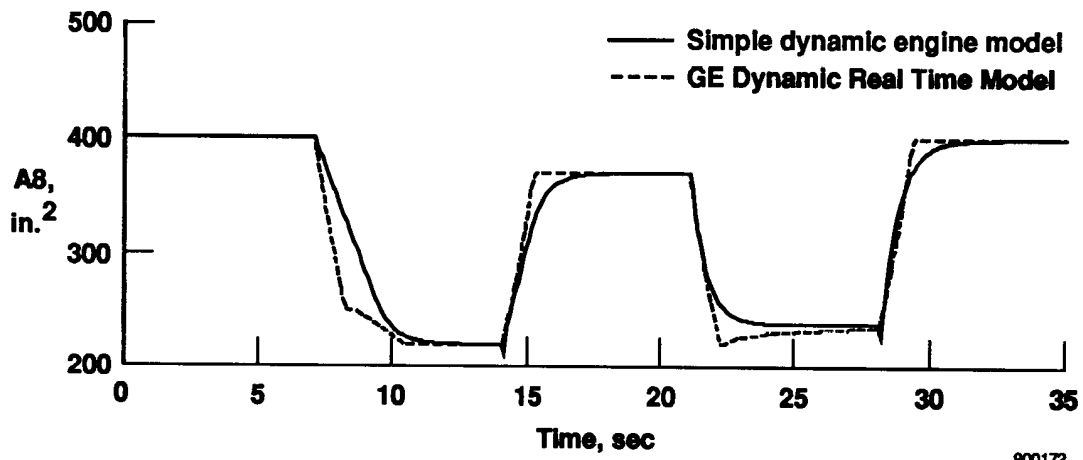
(e) Nozzle throat area comparison.

Fig. 9 Concluded.
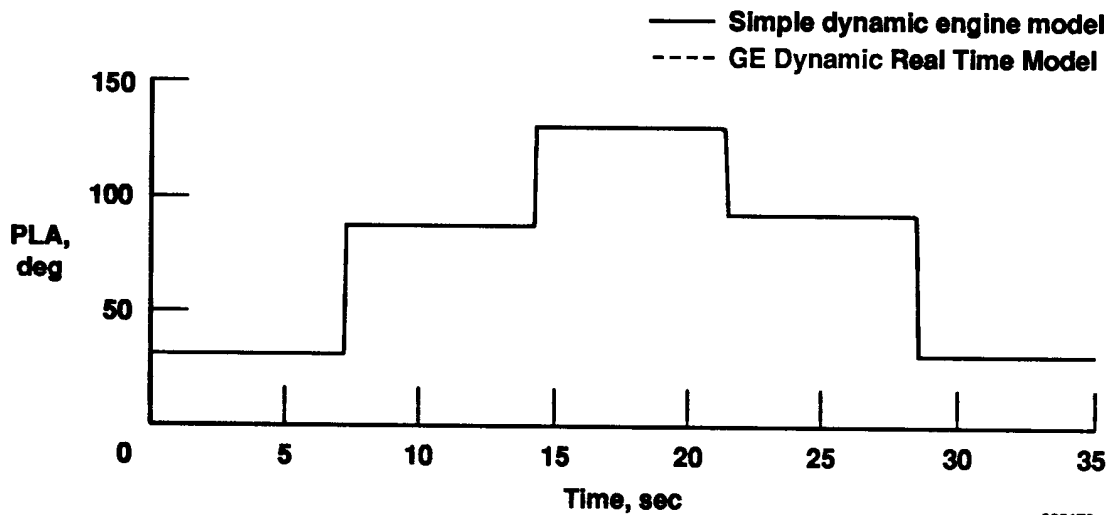
(a) Power lever angle input condition.

Fig. 10 Comparison of the simple dynamic engine model parameters and the GE Model engine parameters, Mach 0.7, H = 35,000 ft, no vectoring.
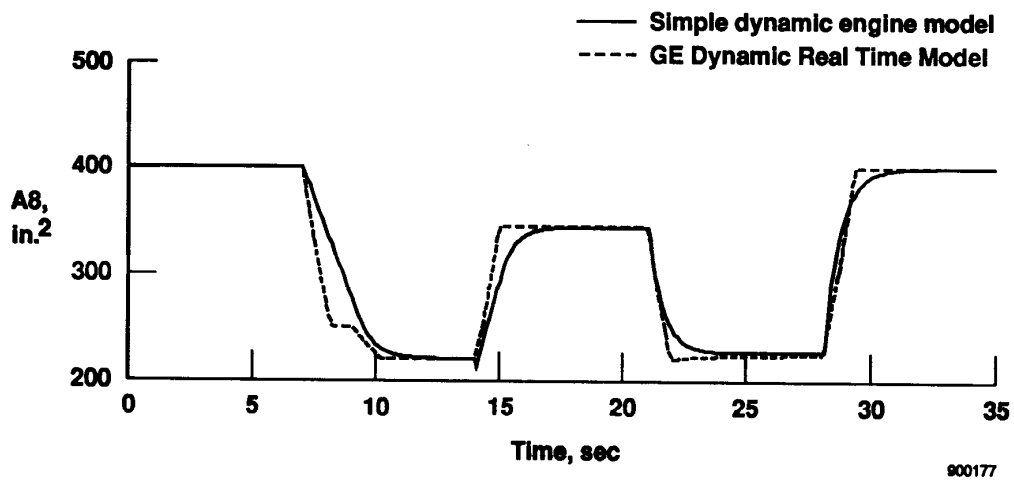
16
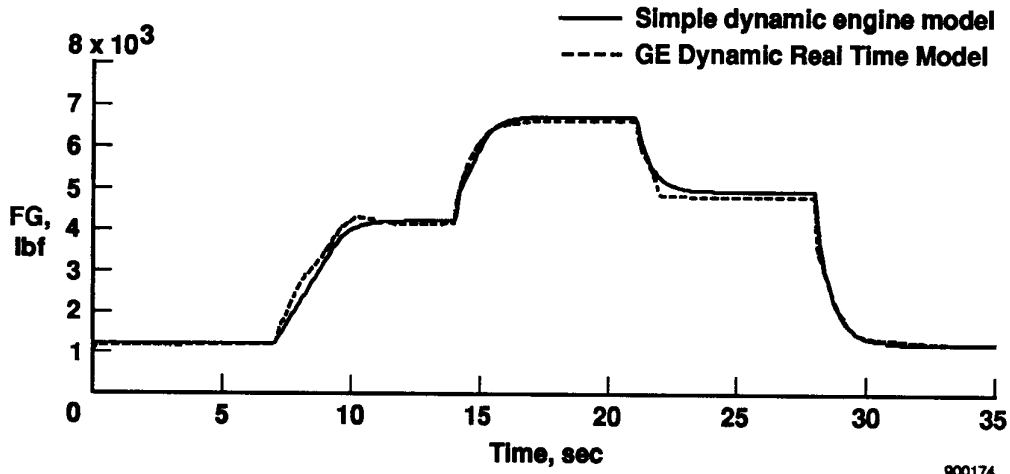
(b) Gross thrust comparison.
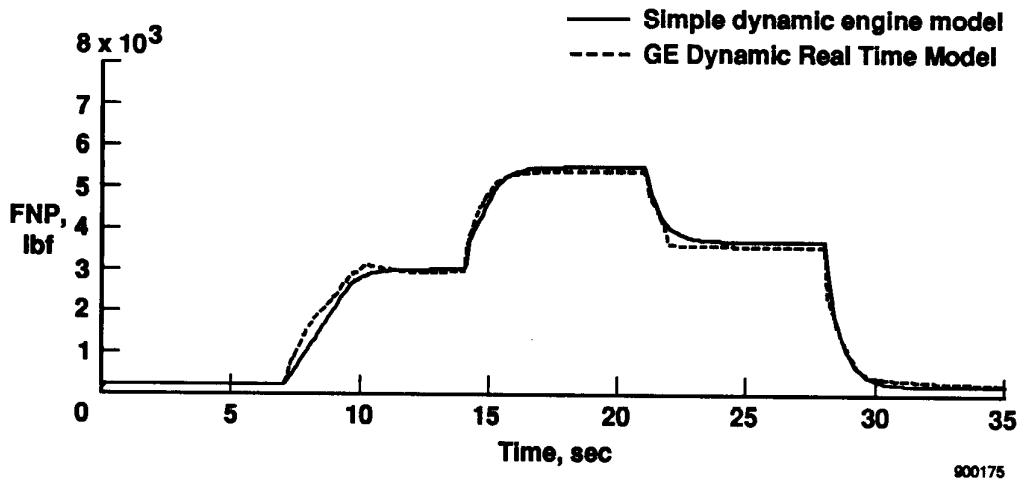
(c) Net propulsive force comparison.

Fig. 10 Continued.

17

(d) Nozzle pressure ratio comparison.

(e) Nozzle throat area comparison.

Fig. 10 Concluded.

18

15. Supplementary Notes

Prepared as AIAA 90-2166 for presentation at the AIAA/SAE/ASME/ASEE Joint Propulsion Conference, Orlando, Florida, July 16–18, 1990.

16. Abstract

A simple dynamic engine model was developed at the NASA Ames Research Center, Dryden Flight Research Facility, for use in thrust vectoring control law development and real-time aircraft simulation. The simple dynamic engine model of the F404-GE-400 engine (General Electric, Lynn, Massachusetts) operates within the aircraft simulator. It was developed using tabular data generated from a complete nonlinear dynamic engine model supplied by the manufacturer. Engine dynamics were simulated using a throttle rate limiter and low-pass filter. This paper includes a description of a method to account for axial thrust loss resulting from thrust vectoring. In addition, this paper presents the development of the simple dynamic engine model and its incorporation into the F-18 high alpha research vehicle (HARV) thrust vectoring simulation. The simple dynamic engine model was evaluated at Mach 0.2, 35,000-ft altitude and at Mach 0.7, 35,000-ft altitude. The simple dynamic engine model is within 3 percent of the steady state response, and within 25 percent of the transient response of the complete nonlinear dynamic engine model.

17. Key Words (Suggested by Author(s)) Aircraft simulation Engine model Real-time simulation Thrust vectoring		18. Distribution Statement Unclassified-Unlimited Subject category - 05
19. Security Classif. (of this report) Unclassified	20. Security Classif. (of this page) Unclassified	21. No. of Pages 24	22. Price A02